NJC

Accepted Manuscript

This is an *Accepted Manuscript*, which has been through the Royal Society of Chemistry peer review process and has been accepted for publication.

Accepted Manuscripts are published online shortly after acceptance, before technical editing, formatting and proof reading. Using this free service, authors can make their results available to the community, in citable form, before we publish the edited article. We will replace this *Accepted Manuscript* with the edited and formatted *Advance Article* as soon as it is available.

You can find more information about *Accepted Manuscripts* in the Information for Authors.

Please note that technical editing may introduce minor changes to the text and/or graphics, which may alter content. The journal's standard Terms & Conditions and the Ethical guidelines still apply. In no event shall the Royal Society of Chemistry be held responsible for any errors or omissions in this *Accepted Manuscript* or any consequences arising from the use of any information it contains.

ROYAL SOCIETY OF CHEMISTRY

www.rsc.org/njc

Organic Charge Transfer Complexes for Selective Accommodation of Aromatic Isomers Using Anthracene Derivatives and TCNQ

Arshad Khan [a], Mingliang Wang*[a], Rabia Usman[a], Jiao Lu [a], Hao Sun [a], Man Du [a], Ruimin Zhang [a], , Chunxiang Xu [b]*

† *School of Chemistry and Chemical Engineering, Southeast University, Nanjing 211189, P. R. China*

‡ *State Key Laboratory of Bioelectronics, Southeast University, Nanjing 210096, P. R. China*

*Corresponding author. Tel.: +862585092237. E-mail address: (M.W.) 101010078@seu.edu.cn; (C.X.) xcxseu@seu.edu.cn

ABSTRACT: Four new organic charge transfer complexes (**Ct1, Ct2, Ct3** and **Ct4**) have been engineered via anthracene derivatives namely, acetyl-3-phenyl-5-(9-anthryl)-2-pyrazoline/1-acetyl-3-naphthyl-5-(9-anthryl)-2-pyrazoline as donors and Tetracyanoquinodimetahne as the acceptor by solution crystallization method. The resulting encapsulated charge transfer complexes (**Ct2-Ct4**) characterized by single crystal X-ray diffraction (SCXRD) analysis showed the formation of channels in supramolecular architecture through various non-covalent interactions. Interestingly, **Ct1** has demonstrated remarkable selectivity towards ***p*-xylene** over other xylene isomers to form the **Ct1.*p*-xylene** inclusion complex. **Ct2** and **Ct3** contain ***p*-xylene** whereas, **Ct4** features ***p*-chlorotoulene**. Moreover, the closely matched Powder X-ray diffraction (PXRD) profile revealed that **Ct2** and **Ct1.*p*-xylene** are isomorphic.

Introduction

The term supra molecular chemistry[1, 2] encompasses various non-covalent routes that trigger scientific community to explore macroscopic characteristics in molecular level to get in depth knowledge about various intriguing phenomena. The importance of these interactions can be anticipated from the vast applications in diverse fields of light-emitting diodes[3], solar cells[4] and lasers[5]. Inspired by various intermolecular interactions, scientists utilized hydrogen bonding sites and open metals sites to construct supra molecular frameworks such as Metal-organic frameworks (MOFs)[6] with promising applications in storage[7], separation[8], and catalysis[9]. Among the various non-covalent interactions, charge transfer interactions (CT) is also one of the approach to self-assemble donor-acceptor species via CT as well as hydrogen bonding interactions to fabricate various supra molecular frameworks with exciting properties [10, 11]. In term of directional behavior, CT interactions are regarded as parallel to hydrogen bonding, offering excellent solvent tolerance and easy spectroscopic investigation[12].

Xylene isomers (*o*-xylene (oX), *m*-xylene (mX) and *p*-*x*ylene (pX)) are important raw materials in chemical industrial process. Unfortunately, due to the nearly similar physical characteristics of xylene isomers such as their boiling points it is difficult to separate them completely. Hence, the separation of pX become more and more significant in term of purity, yield, and capacity[13]. Recently, CT complexes have been fabricated which have the ability to encapsulate the solvents in its channels[14, 15]. However, reports about the selective separation of pX by CT complex in scientific literature made no news. Previously, we have designed an organic cocrystal with single to single crystal transformation that can adsorb all the xylene isomers with no preference for a specific isomer[16]. Thus, constructing a CT complex for selective encapsulation of pX driven by charge transfer interactions along with other secondary non-covalent interactions such

as hydrogen-bonding, solvophobic forces become challenging.

In this contribution, we have engineered a donor-acceptor CT complex using anthracene derivatives namely, acetyl-3-phenyl-5-(9-anthryl)-2-pyrazoline (**APAP**)/1-acetyl-3-naphthyl-5-(9-anthryl)-2-pyrazoline (**ANNP**) as donors and Tetracyanoquinodimetahne (**TCNQ**) as acceptor (Scheme. 1), for selective accommodation of aromatics (pX and ***p*-chlorotoulene** (p.ct)) from a mixture of organic solvents to form CT inclusion complexes. All these complexes were analyzed using multiple techniques. We believe the strict selective accommodation of **Ct1** cocrystal may have potential applications in the separation of pX.

Experimental Section

Synthesis of donor compounds. APAP and ANNP were synthesized by using our previously reported protocol [17]. TCNQ (CAS 1518−16−7) was purchased from Alfa and used without further purification. Analytical-grade solvents were used.

Charge Transfer (CT) cocrystals preparation (Ct1-Ct4). CT co-crystals were prepared by solution evaporation method. Co-crystals **Ct1** and **Ct2** were yielded from a 1:1 stoichiometric amount of APAP and TCNQ in DCM/acetonitrile (20 mL, v:v = 1:1) or DCM/pX (20 mL, v:v = 1:1) mixture after four days (Scheme. 2). Crystals of **Ct1** were rod-shaped dark green in colour having diameter 18.8 μm calculated by scanning-electron microscopic (SEM) studies while **Ct2** crystals are black block. Unfortunately, we did not succeed to collect single crystal data of **Ct1** over successive attempts (**^{1}H-NMR** spectra fig S1 in the ESI).

Co-crystals **Ct3** and **Ct4** were grown from a 1:1 stoichiometric amount of ANNP and TCNQ in DCM/pX (20 mL, v:v = 1:1) or DCM/p.ct (20 mL, v:v = 1:1) mixtures. Black block crystals were yielded after four days by slow evaporation at room temperature. The yields of the different CT complexes obtained during the process of crystallization are **Ct1:** 72%, **Ct2:** 66%, **Ct3** 71%**: Ct4:** 69%.

Characterization Studies

PX**RD** patterns for the solids were recorded using a 18KW advance X-ray diffractometer with Cu Kα radiation (λ=1.54056 Å). **Single X-ray diffraction** data for crystals **Ct2-Ct4** were collected on Nonius CAD4 diffractometer with Mo Kα radiation (λ= 0.71073 Å). The structures were solved with direct methods using the SHELXL-2014/7 program and refined anisotropically using full-matrix least-squares procedure[18]. All non-hydrogen atoms were refined anisotropically and were inserted at their calculated positions and fixed at their positions.

^{1}H-NMR spectra were obtained at 303 K on a Bruker Avance 500 MHz NMR spectrometer using $CDCl_3$ as solvent and TMS as internal standard. **DSC** and **thermogravimetric** analysis (TGA) patterns were recorded with a Mettler-Toledo TGA/DSC 1 Thermogravimetric Analyzer with the temperature scanned from 50 to 300 °C at 10 °C /min. **UV-Vis** absorption spectra were collected on a Shimadzu UV-3600 spectrometer. GC experiments were performed by GC 9890A.

RESULTS AND DISCUSSION.

All the CT complexes were harvested by solution crystallization method from APAP/ANNP and TCNQ (1:1) in a mixture of organic solvents followed by subsequent evaporation of solvents at room temperature affording one binary cocrystal (**Ct1**) and three solvates (**Ct2**,**Ct3** and **Ct4**) which were fully characterized by various analytical tools.

Single X-ray diffraction analysis. Crystallographic structural analysis indicate that crystals **Ct2-Ct4** belong to triclinic system and crystallize in $P\bar{1}$ space group including one molecule each of APAP (**Ct2**) and ANNP (**Ct3** and **Ct4**), aromatic isomers and half molecule of TCNQ in an asymmetric unit with different dihedral-angle between pyrazoline ring and anthracene ring which is presented in Table 2. In these crystals, TCNQ molecules become sandwiched between dimeric donor molecules in the three CT complexes via CT interactions, which can be evidenced from

the results of inter-planar distance (dπ-dπ) and the closest centroid distance (dc-dc Table 3). The single x-ray diffraction crystallographic and structure refinement data are summarized in table. 1.

Table 1. Crystallographic Data and Structure refinement details of crystals **Ct2-Ct4**

Crystal	Ct2	Ct3	Ct4
Formula	$C_{39}H_{32}N_4O$	$C_{43}H_{34}N_4O$	$C_{42}H_{32}ClN_4O$
Temperature/K	293	293	293
Crystal size/mm^3	0.30×0.20×0.10	0.30×0.20×0.10	0.30×0.20×0.10
Morphology	Block	Block	Block
Crystal system	Triclinic	Triclinic	Triclinic
Space group	Pī	Pī	Pī
a/ Å	9.928(2)	9.7190(19)	9.899(2)
b/ Å	10.632(2)	10.356(2)	10.339(2)
c/ Å	16.282(3)	17.804(4)	16.807(3)
α/deg	76.58(3)	74.09(3)	100.87(3)
β/deg	72.43(3)	86.73(3)	99.00(3)
γ/deg	77.68(3)	85.69(3)	98.93(3)
V/ Å^3	1574.6(7)	1717.2(7)	1637.9(6)
Z	2	2	2
ρ (calcd)/Mg m^{-3}	1.208	1.204	1.306
θ Range for data collection/°	1.33-25.37	1.19-25.37	1.25 -25.37
F(000)	604	656	674
Ref collected/unique	6138 / 5773	6732/6327	6382 / 6003
R_1, wR_2($I > 2\sigma(I)$)	0.0576, 0.1583	0.0642, 0.1787	0.1445, 0.3293
R_1, w R_2 (all data)	0.0979, 0.1862	0.1192, 0.2047	0.1915, 0.3695
Goodness-of-fit,S	1.038	1.009	1.288
CCDC	1059084	1059085	1059083

Table 2. Dihedral Angles of APAP and ANNP in each Crystal

Crystal	angles(deg)[a]
Ct2	88.70
Ct3	80.94
Ct4	85.85

[a] The dihedral angles between the pyrazoline rings and anthracene rings of the crystallographically independent ANNP and APAP molecules.

Table 3. Face-to-Face π-packing interactions between TCNQ and Anthracene-moieties

Crystal	Interaction	$d_{\pi\text{-}\pi}$, $d_{\text{c-c}}$(Å)[a]	angle (deg)[b]
Ct2	TCNQ···anthracene	3.546, 4.189	5.35
Ct3	TCNQ···anthracene	3.569, 4.305	7.06
Ct4	TCNQ···anthracene	3.652,4.168	8.03

Description of Ct2-Ct4 co-crystals. The framework of the CT complexes are accomplished through various non-covalent interactions (fig. 1) such as CT interactions, C-H···O, C-H···N hydrogen bonds, C-N···π and C-H···π interactions summarized in table 4 – 5. These operative forces among donor-acceptor complexes formed two racemic chains of APAP (**Ct2**) and ANNP (**Ct3** and **Ct4**) which stack together by C-H···π interactions along a-axis between adjacent hetero-chiral chains of APAP and ANNP to form channel like framework. The aromatic isomers were found to have two kinds of orientations in these crystal systems, connecting the neighboring racemic chains of APAP and ANNP and stabilizing the supramolecular framework by van der waals interactions via C-H···π interactions for **Ct2** and **Ct3** and C-H···π interaction and C-Cl···π interactions for **Ct4** (fig 2). Perhaps the most interesting feature of **Ct2-Ct4** crystals structures is their accommodation of linear isomers within the channels that make the framework of these complexes much stable compare to the bent isomers.

Table 4. Inter-molecular Hydrogen Bond in Crystals **Ct2-Ct4**

Crystal	D-H (Å)	H···A (Å)	D···A (Å)	∠D-H···A (deg)
Ct2				
C33-H33A···O	0.930	2.599	3.517	169.02
C38-H38A···O	0.931	2.374	3.227	152.30
C22-H22A···N4	0.930	2.654	3.550	161.93
C10-H10A···O4	0.930	2.399	3.235	149.37
C32-H32A···O4	0.930	3.154	3.791	127.54
Ct3				
C42-H42A···O	0.930	2.384	3.257	156.38
C22-H22A···N4	0.930	2.585	3.367	143.13
C32-H32B···N3	0.961	2.895	3.836	166.48
C34-H34B···N4	0.961	2.895	3.550	102.12
Ct4				
C10-H10A···N4	0.930	2.635	3.511	153.77
C40-H40A···O	0.931	2.351	3.212	153.92
C35-H35A···O	0.930	2.495	3.414	169.90
C34-H34A···N3	0.930	2.939	3.501	120.21

Table 5. C–H···π and C–N···π interactions in Crystals **Ct2-Ct4**

Crystal	Interaction	distance (Å)[a]	angle (deg)[b]
Ct2	C12-H12A··· Benzene	2.837	148.95
	C28-H28A··· anthracene	2.945	117.78
	C7-H7··· Benzene	3.068	168.82
	C16-H16B···Benzene	2.734	145.38
	C16-H16A···pyrazoline	3.151	130.69
	C36-N4···anthracene	3.545	78.78

Ct3	C15-H15A···napthalene	2.894	142.09
	C9-H9A··· Benzene	3.034	168.25
	C16-H16B···Benzene	2.852	129.55
	C40-N4··· anthracene	3.787	76.10
	C32-H32A···anthracene	3.052	128.60
Ct4	C8-H8A··· naphthalene	2.863	143.44
	C1-Cl··· naphthalene	3.895	63.77
	C1-H1A··· naphthalene	3.096	156.22
	C30-H43B··· naphthalene	3.029	129.26
	C30-N4···anthracene	3.524	76.19

[a] The distances were measured from hydrogen or nitrogen atom to the center of the aromatic ring (for C-H···π or C-N···π interactions); [b] The angles were measured between C-H-*c* or C-N-*c* (for C-H···π or C-N···π interactions).

Powder X-ray diffraction (PX**RD) Studies.** The PXRD profiles of these crystals (fig. 3) were consistent with that simulated from SCXRD data structures of **Ct2-Ct4** which affirm phase purity and homogeneity of these complexes. Moreover, the PXRD plot of **Ct1** show different structure comparing to other CT complexes suggesting new phase has been formed with different molecular stacking. PXRD index together with thermal properties on these CT complexes are good indicators to investigate different crystalline forms.

Thermal Measurements. For crystal **Ct1**, DSC (fig 4) exhibit one peak at 240 °C confirming that the crystal belongs to single component system. TGA thermogarm of **Ct2** showed the weight loss (18.13%) in the temperature range from 120 °C to 145 °C. Thus, the first endotherm is ascribed to the removal of pX molecules and the weight loss coincides with the theoretical weight loss (18.53%) of **Ct2** and the second endotherm at around 208 °C (β form), which appeared after the de-solvation endotherm and just before the melting at around 235 °C (γ form), indicating the phase transformation in **Ct2.** The results of the DSC studies displayed two

endothermic peaks observed at 144 ^{o}C and 138 ^{o}C for **Ct3** and **Ct4** complexes, attributed to the release of aromatic isomers (pX and p.ct) from the crystal system and melting of residual solids respectively. In TGA measurement the weight released for crystals of **Ct3** and **Ct4** were 16.43% and 19.01% respectively, which is consistent with the theoretical weight losses which were 17.04% and 19.69%respectively (fig 4). In summary, DSC and PXRD patterns measured for **Ct1-Ct4** can be used to identify the different forms of these co-crystals.

Spectroscopic Measurements

Solid-state absorption studies of CT complexes. Solid state absorption spectroscopy was performed for donor-acceptor complexes to explore the formation of CT cocrystal[19]. As shown in fig 5, all the CT complexes showed a new broad absorption band in the range of 650-790 nm, compare to their parent components which did not display such bands, indicating that CT interactions do have effect on the CT system. The CT complexes have a strong absorption band that extends to near infrared region, making the crystals to appear black.

FTIR-Spectroscopy. As illustrated in fig 6, small notable changes in (C≡N) vibration frequency were observed during IR-spectra measurement. In free or neutral state, TCNQ showed a strong vibration peak at 2223cm^{-1} corresponding to (C≡N) stretching which shift to lower frequency upon CT complexation. In **Ct1-Ct2** and **Ct-Ct4**, the peaks corresponding to the C≡N stretching were appeared at 2219 cm^{-1}, 2216 cm^{-1}, 2215 cm^{-1} and 2219 cm^{-1} respectively, which obviously emphasize the presence of distinct CT interactions between APAP/ANNP and TCNQ. Similarly, the bands assigned to C=O in APAP/APAP (1668 cm^{-1}) showed a red shift of 2-8 cm^{-1} in CT complexes (Ct1: 1660 cm^{-1}, Ct2: 1666 cm^{-1}, Ct3: 1666 cm^{-1} and Ct4: 1660 cm^{-1}) which can be attributed to CT effect and the different π-π stacking in these CT complexes. The results of

vibrational spectroscopy strongly support the formation of CT complexes. (Raman spectra, Fig. S2 in the ESI).

Selective-Accommodation Experiment. To explore the feasibility of **Ct1** for selective accommodation, 100 mg of **Ct1** was directly immersed into an equimolar mixture of solvents oX/pX, pX/mX, oX/mX (200 µl), or exposing to pure isomers (100 µl) alone in sealed glass vial for 10 hours at room temperature, where it showed selective discrimination and took up pX. The pX uptake by **Ct1** is established by ^{1}H-NMR (Fig S3 in the ESI) and GC measurement.

Adsorption preference of **Ct1** for pX was first carried out by a screening series of batch competitive experiments through GC investigation. Owing to the closely matched retention time of mX and pX (Fig 7b), GC chromatogram depicts one signal. To further establish whether the observed decrease in the concentration of pX is only due to sole effect of pX not mX, we performed the GC measurement on oX/mX mixture. GC chromatogram confirms that the observed decrease in the concentration of pX is attributed to the **Ct1** affinity for pX not mX (Table. 6). Comparing with the calculated value of pX for **Ct2 (**26.45%), the amount of pX adsorbed by the respective mixtures based on the analysis of the GC measurement are 26.05% in pX/oX and 27.10% in pX/oX/mX respectively (Table 6).

Table 6. Selectivities permeates calculated from GC data for **Ct1**

Entry	Before addition	After addition
Content of pX (%) in pX/oX	46.11	38.82
Content of mX and pX (%) in pX/mX/oX	64.64	61.33
Content of mX (%) in mX/oX	48.57	49.09
Content of oX (%) in mX/oX	51.39	50.87

The potential ability of **Ct1** to effectively screen pX was further proven by analyzing the solids via PXRD and DSC/TGA tests. PXRD plots (Fig. 8) of **Ct1** in pX, oX/pX and mX/pX are same with **Ct2,** indicative of the fact that **Ct1** does has affinity for pX to generate **Ct1.pX**.

Experimental TGA traces agree well with the theoretical weight loss of all the CT complexes in different solutions mixtures (Table. 7). Differential scanning calorimetry (DSC) of **Ct1** in pX, oX/pX and mX/pX mixtures and that of **Ct2** reveal an endothermic peak at 114 ^{o}C, 130 ^{o}C 131 ^{o}C, and 131 ^{o}C, respectively, which is due to the loss of pX from the crystal structure thereby proven the contention that **Ct1** does adsorb pX (Fig. 9). Moreover, it can be seen from DSC for **Ct1.pX,** the peak of losing pX appeared earlier compare to other samples and the weight loss of pX from sample of **Ct1.pX** is 14.85%, obviously less than that of theoretical weight loss (18.54%) owing to little amount of pX was used in the experiment. To further support our selectivity phenomena, we immersed **Ct1** in a mixture of oX/mX and remarkably we found a single endotherm which is attributed to the melting of **Ct1** crystal, indicating no affinity of **Ct1** towards mX. The results of PXRD and thermal analysis of the CT complexes contribute to the structural mimicry of **Ct1.pX** and **Ct2** and thus we may speculate that **Ct1.pX** and **Ct2** may share the same interaction and packing mode.

Table 7. Detail thermal data (DSC/TGA) of **Ct1** for selective adsorption of **pX**

Sample	Theoretical weight loss (%)	Exp weight loss (%)
Ct2	18.539	18.592
Ct1+pX		14.850
Ct1+pX+mX		18.786
Ct1+pX+oX		18.034

We also have performed desorption experiment by heating the crystal **Ct1.pX** in oven at 150ºC for 2 hours at normal pressure. Strikingly, powder X-ray diffraction (PXRD) plot of the

desolvated crystals (Fig. 10) were found to be in good agreement with that of crystal **Ct1** suggesting that **Ct1** may have potential applications in the separation and purification of pX. Furthermore, it can be also seen from the PXRD pattern that the crystals of **Ct1.pX** are thermally stable and did not undergoes remarkable structural transformation. Similarly, PXRD results of desolvation of **Ct3** and **Ct4** demonstrated that the products are stable even after the removal of solvents (Figure S4 in the ESI).

We assume the strict selection of pX by **Ct1** over the other xylene isomers is may be attributed to the molecular dimension i,e allow only the inclusion of linear molecule, pX not the bent one such as oX and mX[20].

CONCLUSION

In summary, we have designed charge-transfer complexes from anthracene derivatives using donor-acceptor chemistry that formed supramolecular channels to accommodate aromatic isomers. The supramolecular systems were held together by collaborative hydrogen bonding, C-H$\cdots\pi$, $\pi\cdots\pi$ bonds etc. All these three complexes exhibited similar crystal structures with slit like channels and stabilized by linear aromatic isomers present in the channels. Single crystal X-ray diffraction, Infrared and solid state Ultraviolet spectroscopy analysis confirm presence of charge transfer interactions in all the crystal structures. Interestingly, crystals of **Ct1** demonstrated strict selectivity for *p*-xylene over other two isomers generating **Ct1.*p*-xylene** complex, established through Gas Chromatography, powder X-ray diffraction studies, differential scanning calorimetry and thermogravimetric measurements. The unique feature of selective accommodation of *p*-xylene by **Ct1** complex makes it a novel potential candidate for separation and purification of xylene isomers.

ACKNOWLEDGMENT

The authors acknowledge the support of National Basic Research Program of China (2011CB302004).

REFERENCES

1. R. K. Castellano and J. Rebek, *Journal of the American Chemical Society*, 1998, **120**, 3657-3663.
2. H. S. Freeman, *Journal of the American Chemical Society*, 2006, **128**, 6521-6521.
3. R. H. Friend, R. W. Gymer, A. B. Holmes, J. H. Burroughes, R. N. Marks, C. Taliani, D. D. C. Bradley, D. A. D. Santos, J. L. Bredas, M. Logdlund and W. R. Salaneck, *Nature*, 1999, **397**, 121-128.
4. T. Horiuchi, H. Miura, K. Sumioka and S. Uchida, *J Am Chem Soc*, 2004, **126**, 12218-12219.
5. C. Zhang, C.-L. Zou, Y. Yan, R. Hao, F.-W. Sun, Z.-F. Han, Y. S. Zhao and J. Yao, *Journal of the American Chemical Society*, 2011, **133**, 7276-7279.
6. J. E. Warren, C. G. Perkins, K. E. Jelfs, P. Boldrin, P. A. Chater, G. J. Miller, T. D. Manning, M. E. Briggs, K. C. Stylianou, J. B. Claridge and M. J. Rosseinsky, *Angewandte Chemie International Edition*, 2014, **53**, 4592-4596.
7. G. Férey, C. Mellot-Draznieks, C. Serre, F. Millange, J. Dutour, S. Surblé and I. Margiolaki, *Science*, 2005, **309**, 2040-2042.
8. J. S. Seo, D. Whang, H. Lee, S. I. Jun, J. Oh, Y. J. Jeon and K. Kim, *Nature*, 2000, **404**, 982-986.
9. C.-D. Wu, A. Hu, L. Zhang and W. Lin, *Journal of the American Chemical Society*, 2005, **127**, 8940-8941.
10. M. Kurmoo, A. W. Graham, P. Day, S. J. Coles, M. B. Hursthouse, J. L. Caulfield, J. Singleton, F. L. Pratt and W. Hayes, *J. Am. Chem. Soc.*, 1995, **117**, 12209.
11. Q. Liao, H. Fu, C. Wang and J. Yao, *Angewandte Chemie International Edition*, 2011, **50**, 4942-4946.
12. A. Das and S. Ghosh, *Angewandte Chemie International Edition*, 2014, **53**, 2038-2054.
13. H. Jobic, A. Méthivier and G. Ehlers, *Microporous and Mesoporous Materials*, 2002, **56**, 27-32.
14. O. Kataeva, M. Khrizanforov, Y. Budnikova, D. Islamov, T. Burganov, A. Vandyukov, K. Lyssenko, B. Mahns, M. Nohr, S. Hampel and M. Knupfer, *Crystal Growth & Design*, 2015, DOI: 10.1021/acs.cgd.5b01301.
15. H. Sun, M. Wang, X. Wei, R. Zhang, S. Wang, A. Khan, R. Usman, Q. Feng, M. Du, F. Yu, W. Zhang and C. Xu, *Crystal Growth & Design*, 2015, **15**, 4032-4038.
16. X. Wu, M. Wang, M. Du, J. Lu, J. Chen, A. Khan, R. Usman, X. Wei, Q. Feng and C. Xu, *Crystal Growth & Design*, 2015, **15**, 434-441.
17. M.-L. Wang, B.-L. Dong and Y.-H. Li, *Acta Crystallographica Section E: Structure Reports Online*, 2011, **67**, o94-o94.

18. G. M. Sheldrick, *SHELXS97: Programs for Crystal Structure Analysis, University of Göttingen, Germany*.
19. R. J. Dillon and C. J. Bardeen, *The Journal of Physical Chemistry A*, 2012, **116**, 5145-5150.
20. R. Krishna, *Physical Chemistry Chemical Physics*, 2015, **17**, 39-59.

Scheme 1. Chemical Structure of ANNP and APAP

Scheme 2. Schematic formation of **Ct1**-**Ct4** cocrystals. Solvent moleculs are shown in violet yellow and lime colors in **Ct2-Ct4**.

Figure 1. View of the X-rays crystal structure of **Ct2-Ct4**. Solvent moleculs are shown in pink, orange and cyan colors and hydrogen atoms are not shown for clarity.

Figure 2. Crystal structure showing interframework-solvent interactions in crystals of a) **Ct2** b) **Ct3** and c) **Ct4** complexes. The solvent molecules in **Ct3** are disordered at two positions with occupancy 0.275 and 0.725 and in Ct4 solvent molecule possess inversion of symmetry element.

Figure 3. Simulated (blue) experimental (black) and PXRD overlay of crystals **Ct2-Ct4** except **Ct1**

Figure 4. DSC/ TGA profiles of crystals **Ct1-Ct4**

Figure 5. Solid state absorption spectra of Charge transfer complexes **Ct1-Ct4**

Figure 6. Vibrational spectra of crystals **Ct1-Ct4**

Figure 7. Chromatographic separation of pX (a) Selective uptake of pX from mixture of pX/oX (b) GC chromatogram of mixture of pX/mX/oX solutions. Signals of pX/mX superimposed on each other (c) GC chromatogram of mixture of mX/oX solution excluding pX

Figure 8. Comparative PXRD plots of **Ct1** with mixture of xylene isomers showing selective uptake of pX

Figure 9. Comparing DSC/TGA of crystal **Ct1** for selective accommodation of pX in presence of xylene mixture

Figure 10. PXRD patterns of crystal **Ct1.pX** before and after desolvation

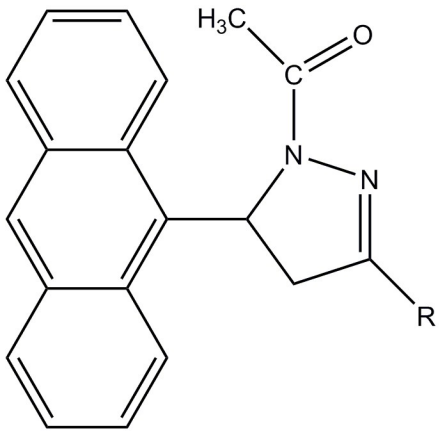

APAP: R=Ph
ANNP: R=Naphthyl

Scheme 1

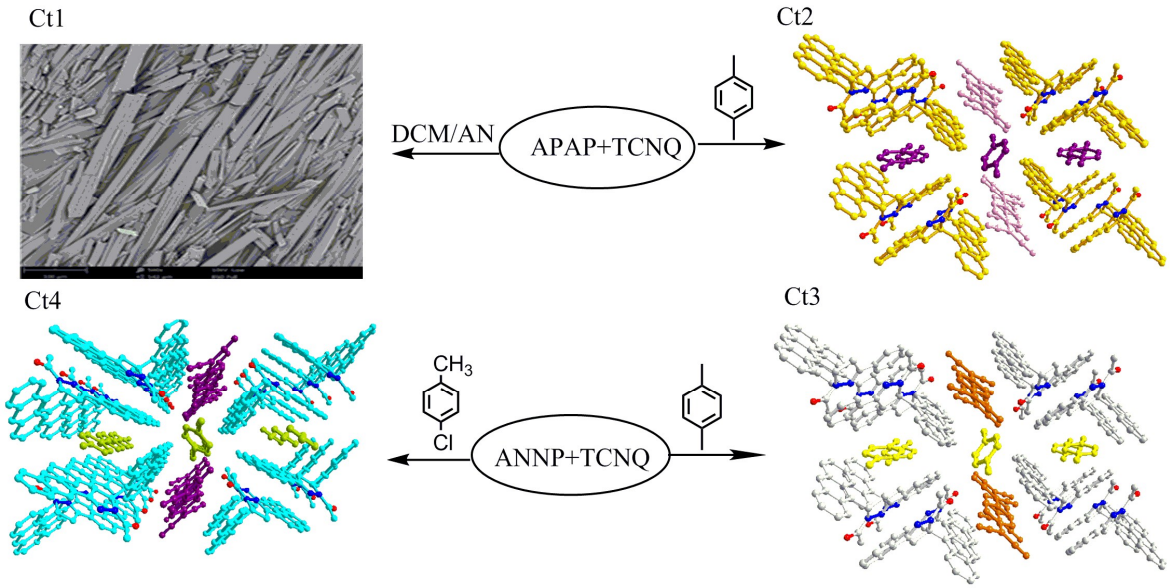

Scheme 2

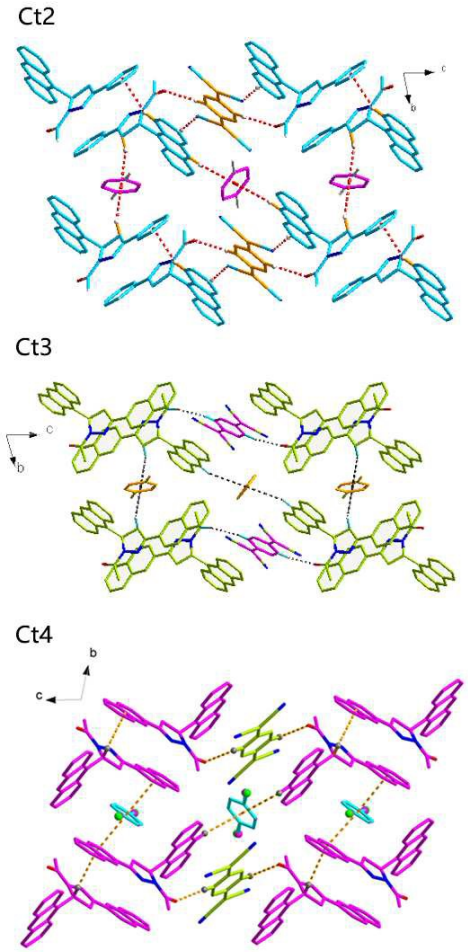

Figure 1

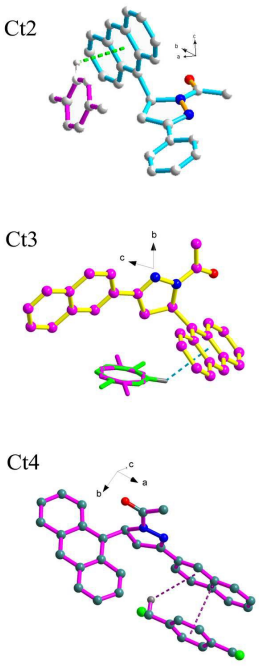

Figure 2

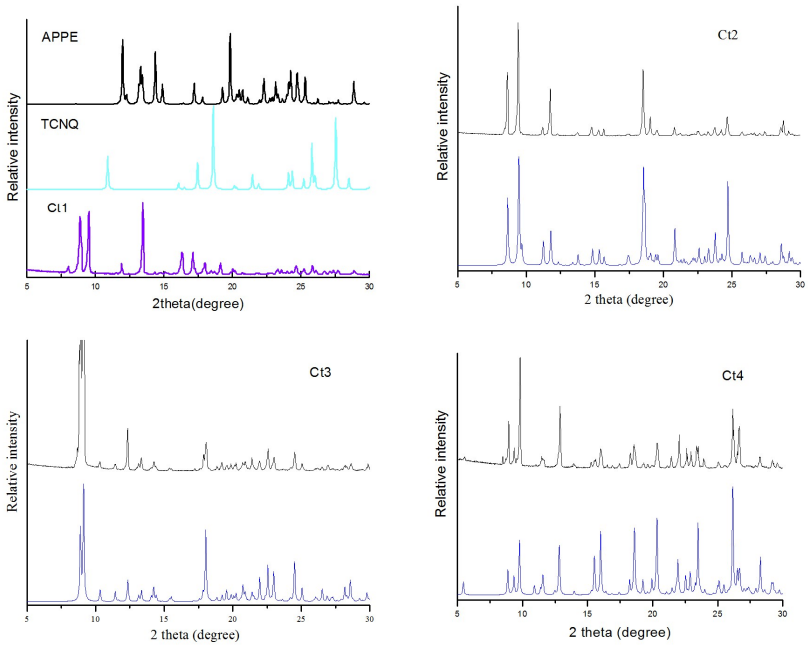

Figure 3

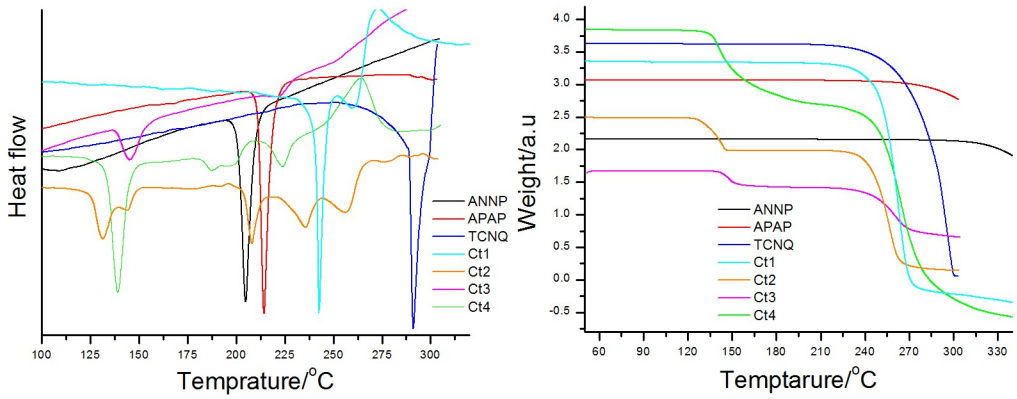

Figure 4

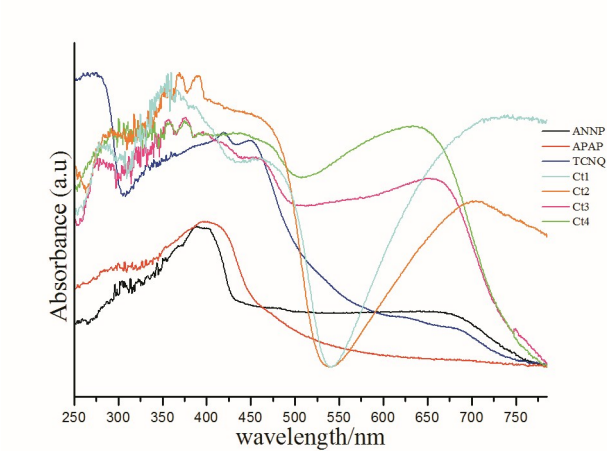

Figure 5

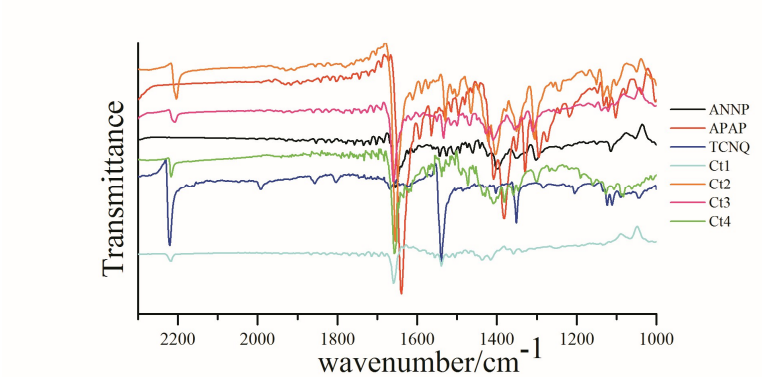

Figure 6

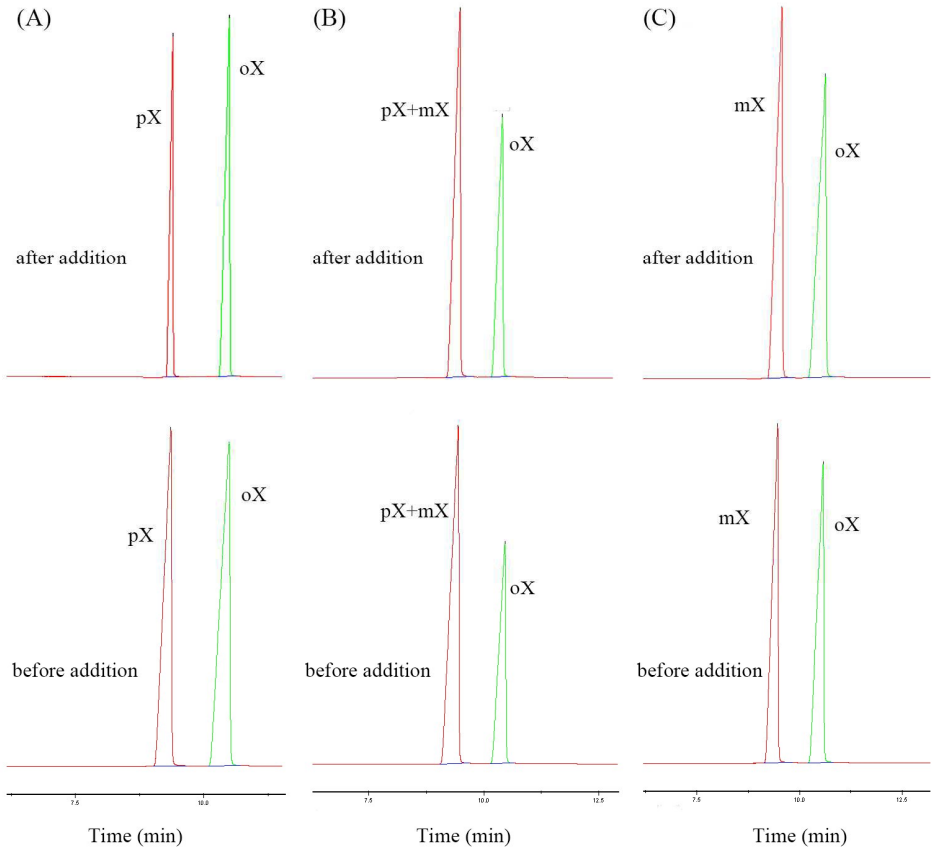

Figure 7

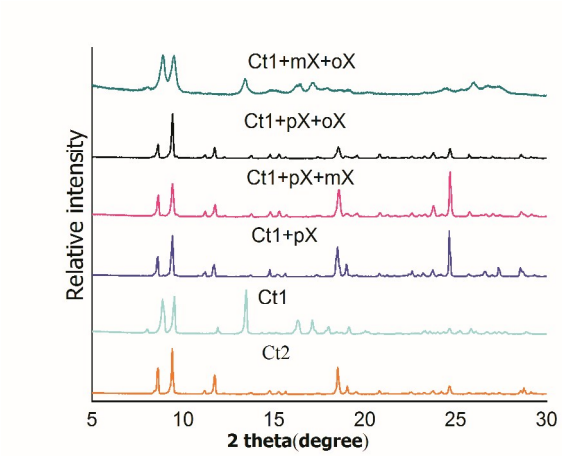

Figure 8

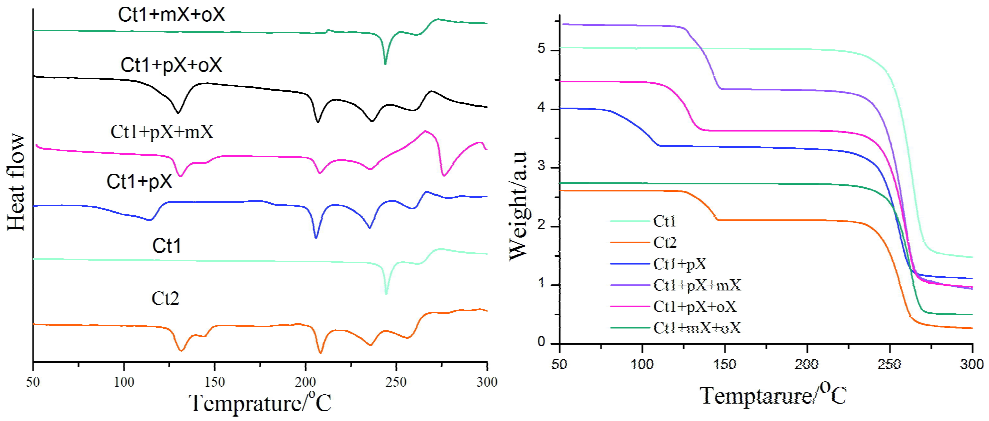

Figure 9

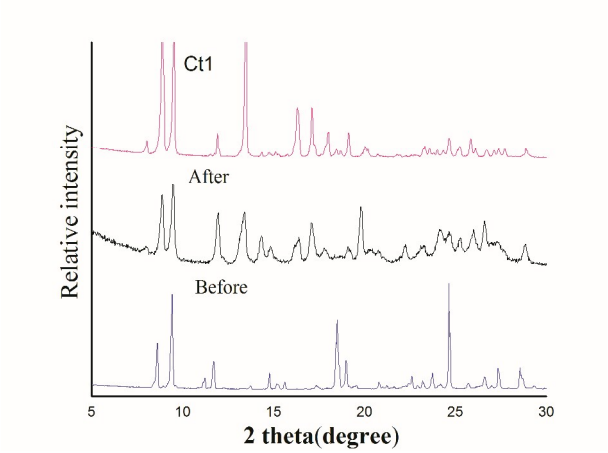

Figure 10

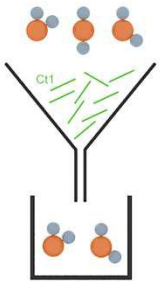

Four Organic-charge transfer (CT) complexes (**Ct1-Ct4**) have been reported. **Ct1** discern p-xylene in presence of xylene mixture.